HAL
open science

Extension of the ICRF for selected areas down to the 16th magnitude – II

J. I B Camargo, C. Ducourant, R. Teixeira, J.-F. Le Campion, M. Rapaport, P. Benevides-Soares

To cite this version:

J. I B Camargo, C. Ducourant, R. Teixeira, J.-F. Le Campion, M. Rapaport, et al.. Extension of the ICRF for selected areas down to the 16th magnitude – II. Astronomy and Astrophysics - A&A, 2003, 409 (1), pp.361-368. 10.1051/0004-6361:20031063 . insu-03324792

HAL Id: insu-03324792

https://insu.hal.science/insu-03324792v1

Submitted on 24 Aug 2021

HAL is a multi-disciplinary open access archive for the deposit and dissemination of scientific research documents, whether they are published or not. The documents may come from teaching and research institutions in France or abroad, or from public or private research centers.

L'archive ouverte pluridisciplinaire **HAL**, est destinée au dépôt et à la diffusion de documents scientifiques de niveau recherche, publiés ou non, émanant des établissements d'enseignement et de recherche français ou étrangers, des laboratoires publics ou privés.

A&A 409, 361–368 (2003)
DOI: 10.1051/0004-6361:20031063
© ESO 2003

Astronomy & Astrophysics

Extension of the ICRF for selected areas down to the 16th magnitude – II⋆,⋆⋆

J. I. B. Camargo[1,2], C. Ducourant[1,2], R. Teixeira[1,2], J.-F. Le Campion[1], M. Rapaport[1], and P. Benevides-Soares[1,2]

[1] Observatoire de Bordeaux, UMR 5804, CNRS/INSU, BP 89, 33270 Floirac, France
[2] Instituto de Astronomia, Geofísica e Ciências Atmosféricas da Universidade de São Paulo, Caixa Postal 3386, 01060-970 São Paulo SP, Brazil

Received 9 April 2003 / Accepted 4 June 2003

Abstract. In this paper we provide a major upgrade of the work presented in Camargo et al. (2001), aiming at the extension of the ICRF at optical wavelengths in regions of special astronomical interest, using observations from the Bordeaux and Valinhos meridian circles. Along with the new fields, the main differences, when compared to the first release, are: a much larger sky coverage, the replacement of the AC2000 by its upgraded version AC2000.2 as one of the first epoch astrometrical sources, inclusion of Tycho–2 and 2MASS⋆⋆⋆ photometry when available, and the correction for a magnitude equation on the Valinhos right ascension system as well. The resulting catalogue contains 678 828 entries with positional external precisions, on both coordinates, ranging from 50–60 mas ($V \leq 13.5$) to 70–140 mas ($13.5 < V \leq 16.0$). For the proper motions, precisions range from 3 mas/year to about 15 mas/year, depending on magnitude and declination.

Key words. astrometry – reference systems

1. Introduction

One of the most important tasks of astrometry rests upon the adoption of a concept and the materialisation of a celestial reference system, from which one can derive the positions of heavenly bodies as well as study their variations as a function of time.

The corresponding celestial reference frame is given by a catalogue containing the coordinates of reference points along with other parameters, so that it is possible for the user to materialise the reference system at any given epoch.

Three characteristics are important for such a reference frame. They are *inertiality*, *rigidity* and *accessibility*. Briefly speaking, *inertiality* can be understood as non-rotation of the coordinate axes, *rigidity* relates to the agreement between the coordinate axes materialised by any subset of the reference frame, and *accessibility* is achieved by the appropriate availability of reference points in the sky, so that the user can use a suitable number of such points in a sky region. This work is concerned mainly with this last topic.

A major breakthrough in astronomical reference systems was achieved with the adoption by IAU, as from 1st of January 1998, of the ICRS (International Celestial Reference System) (Feissel & Mignard 1998; Ma et al. 1998; Johnston & de Vegt 1999), as the celestial reference system to replace the FK5 (Fricke et al. 1988). The ICRS is materialised by a set of 212 extragalactic compact radio sources listed in the ICRF (International Celestial Reference Frame) (Ma et al. 1998). The positions of these sources have been precisely determined by VLBI techniques to accuracies better than 0.5 mas.

In optical wavelengths, the ICRS is realised by the HIPPARCOS catalogue (ESA 1997) with astrometrical parameters for about 118 000 objects, typically brighter than $V = 10.0$ (completeness up to $V = 8.0$), distributed all over the sky. This gives a star density of about 3 objects per square degree, which is insufficient to provide a desirable accessibility to the ICRS. The improvement given by the Tycho–2 catalogue notwithstanding (∼50 stars per square degree and limiting magnitude $V = 12.5$ – completeness up to $V = 11.0$), small field astrometry has still its density needs unfulfilled.

A worldwide effort is in progress to extend the ICRF in optical wavelengths from ground-based observations, supported by the IAU Commission 8 new working-group The "Future

Send offprint requests to: J. I. B. Camargo,
e-mail: camargo@obs.u-bordeaux1.fr

⋆ Based on observations made with the CCD meridian circle at the Bordeaux Observatory, Floirac – France. Based on observations made with the CCD meridian circle at the Abrahão de Moraes Observatory, Valinhos – Brazil. Based on measurements made with the MAMA automatic measuring machine.

⋆⋆ Table 2 is only available in electronic form at the CDS via anonymous ftp to cdsarc.u-strasbg.fr (130.79.128.5) or via http://cdsweb.u-strasbg.fr/cgi-bin/qcat?J/A+A/409/361, and Tables 1 and 3 are only available in electronic form at http://www.edpsciences.org

⋆⋆⋆ This paper was prepared before the release of the all-sky 2MASS survey.

Article published by EDP Sciences and available at http://www.aanda.org or http://dx.doi.org/10.1051/0004-6361:20031063

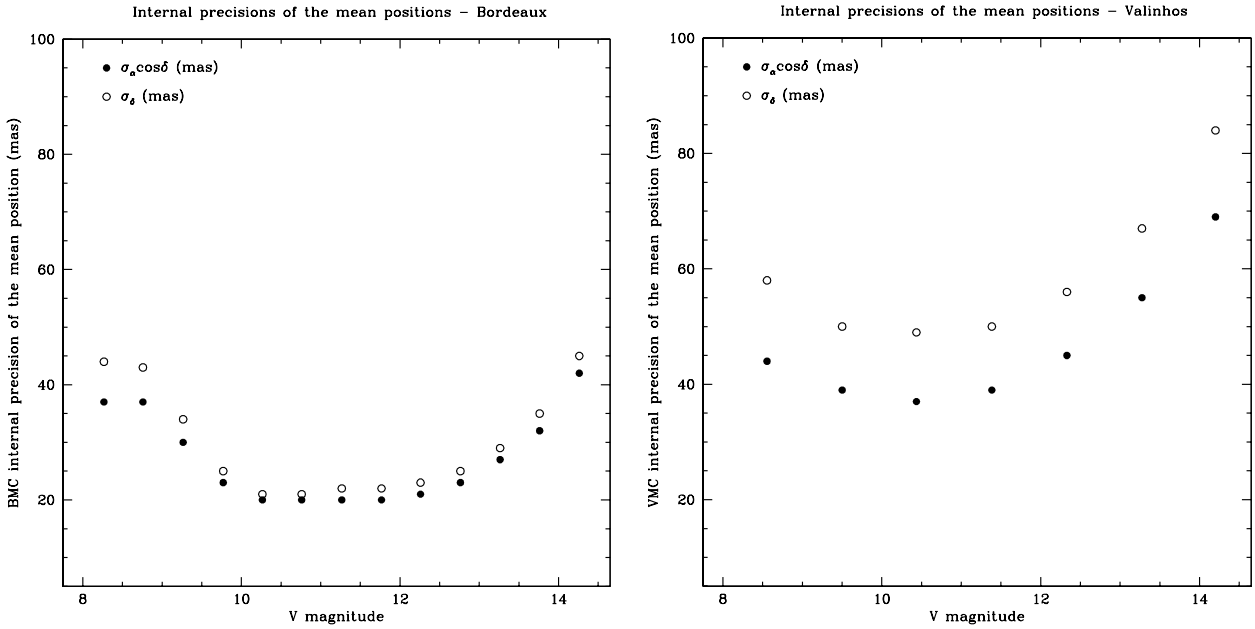

Fig. 1. Internal precisions of the mean positions of the Bordeaux and Valinhos meridian observations.

Development of Ground-Based Astrometry". Examples of such an effort are the USNO–A2.0 catalogue (Monet et al. 1998), UCAC project (Zacharias et al. 2000), A Catalogue of Faint Reference Stars in 398 Fields of Extragalactic Radio Reference Frame Sources – ERLcat (de Vegt et al. 2001), Valinhos Meridian Circle Catalogue – VMCC (Camargo et al. 2001), and M2000 (Rapaport et al. 2001) among others.

The present work is part of this effort and upgrades its previous version, the VMCC. The main differences are: a) observational data now provides 511 525 objects from the Bordeaux CCD meridian circle (hereinafter BMC) and 167 303 objects from the Valinhos CCD meridian circle (hereinafter VMC) – only BMC data was retained whenever common objects between both instruments were detected. VMC data from Camargo et al. (2001), as will be discussed in Sect. 3.2, was reanalysed for this present work; b) Tycho–2 B and V photometry have been included in the catalogue, as well as c) J, H, K photometry from 2MASS; d) correction for a magnitude equation present in the Valinhos right ascension system, and e) replacement of AC2000 by its upgraded version AC2000.2 (Urban et al. 2001) as one of the first epoch sources for proper motion measurements.

Also, in our catalogue (hereinafter BVMCcat) we provide: mean J2000 positions and respective epochs, proper motions, V[1] magnitude from the meridian observations, internal precisions for the astrometric parameters, time interval for proper motion determination, number of meridian observations as well as the involved current and first epoch sources.

2. The meridian circles

The main characteristics of the BMC and VMC have already been described by various papers (Viateau et al. 1999; Dominici et al. 1999; Camargo et al. 2001; Rapaport et al. 2001), and details about both of them can be found in Viateau et al. (1999).

Their locations are, respectively, Floirac (λ = 00°31′39″(east), ϕ = +44°50′07″) in France, and Valinhos (λ = 46°58′03″(west), ϕ = −23°00′06″) in Brazil. Both instruments use CCDs operating in drift scan mode, and the bandpass, 5200 Å to 6800 Å, makes the resulting photometric band close to the Johnson's V band system (Dominici et al. 1999).

The limiting magnitude is about $V = 17.0$ for the BMC and one magnitude brighter for the VMC, due to the larger CCD of the BMC. The internal precision of the mean positions, as a function of magnitude, is shown in Fig. 1. From those panels, it is possible to notice the better performance (about 20 mas) of the BMC compared to that of the VMC. This is explained by the different size of the CCDs, allowing a longer integration time for the BMC, as well as slight differences in the reduction parameters used in each one (ponderation of observations, eliminations). It is also possible to notice a difference (about 10 mas) between the precisions of the right ascension and declination systems presented by the VMC, the origin of which is under investigation. Left and right panels of Fig. 1 are given within the optimal range of magnitude for the instrumental measurements (Viateau et al. 1999).

3. Astrometric data

3.1. Current epoch observations and reduction

Our observational data comprises 242 meridian strips (see Table 1 and Fig. 2), whose declination heights are 28′ for Bordeaux and 13′ for Valinhos, most of them centered on extragalactic radio sources, to support programs devoted to detecting their photometric variability as well as the determination of their optical position from larger telescopes. Also, strips

[1] In this work, no check for variability was performed.

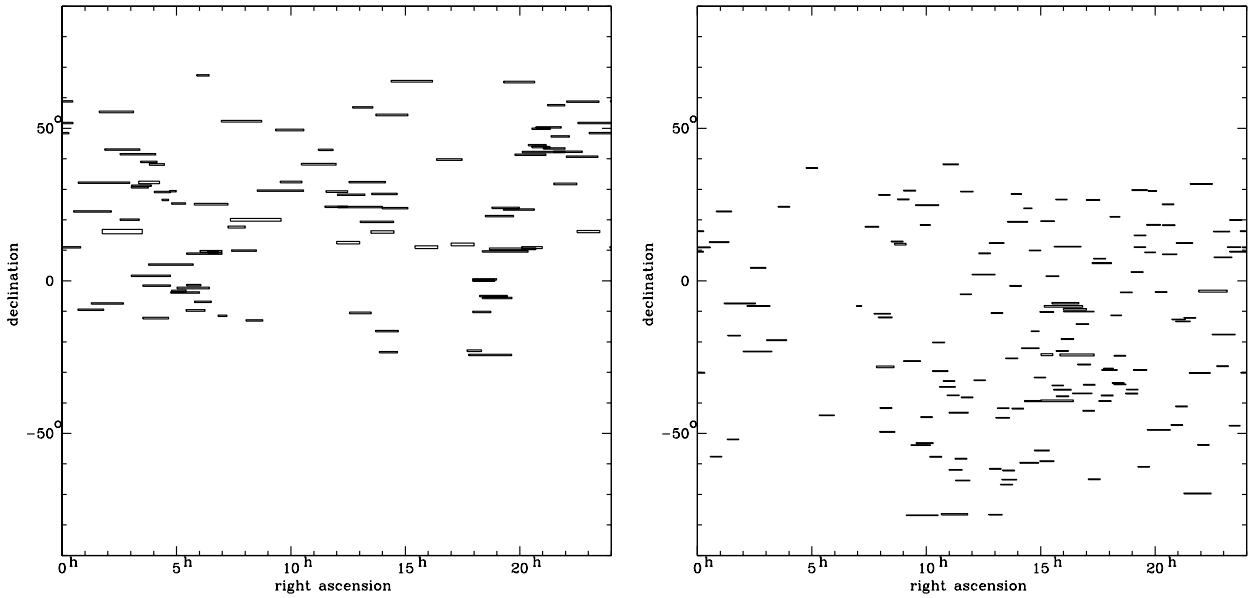

Fig. 2. Distribution of the observations in the sky as given by Bordeaux (left) and Valinhos (right). All overlapping zones were previously treated, in order to eliminate redundant entries from the BVMCcat. The adopted procedure was to retain only the BMC observation whenever an object was observed by both BMC and VMC.

containing pre-main sequence stars observed in the great southern star-forming regions (Chamaeleon, Lupus and Upper Scorpius – Ophiuchus) (Teixeira et al. 2000) and other strips containing regions of young stars, open clusters and Pluto were also included in this data set. All meridian images have been reduced (Viateau et al. 1999), for astrometry and photometry, with the Tycho–2 catalogue.

3.2. Magnitude equation

The presence of a magnitude equation was found on the right ascension system of the Valinhos observations, and corrected according to the curve depicted in Fig. 3, upper panel, before the determinations of the results presented here, that is, before the necessary treatment to build the BVMCcat.

This feature should be compared to the colour dependence found in Bordeaux (Rapaport et al. 2001), the cause of both effects probably being the same. It is a parallax error arising from out-of-focus images caused by the axial spread of the focal plane as a function of the wavelength. The consequent errors are essentially colour dependent. Magnitude dependence arises through the centering algorithms, which include the maximum possible number of pixels, so that bright objects will reflect the influence of the out-of-focus chromatic halo, which is not detected in the case of faint objects (Benevides-Soares 2003).

Further colour dependence effects on the meridian positions were not corrected since colour indexes were not available for all stars. No magnitude equation was found in the BMC observations.

3.3. First and intermediate epoch material

Positions and proper motions presented here were derived from the combination of the present epoch data (BMC and VMC observations) with the aid of almost the same ancient epoch astrometric catalogues presented in Camargo et al. (2001), and following the same procedures. The main differences are the use of the AC2000.2 instead of its previous version, the AC2000 (Urban et al. 1998), and the elimination of those observational data with standard deviations larger than 250 mas in either coordinates. When a given object observed by either the BMC or the VMC had its set of counterparts identified from the first epoch material, no elimination was done on this set. This is also different from the adopted procedure in Camargo et al. (2001). In this work, AC2000.2 precisions were taken from the individual plate solutions (Urban et al. 1998).

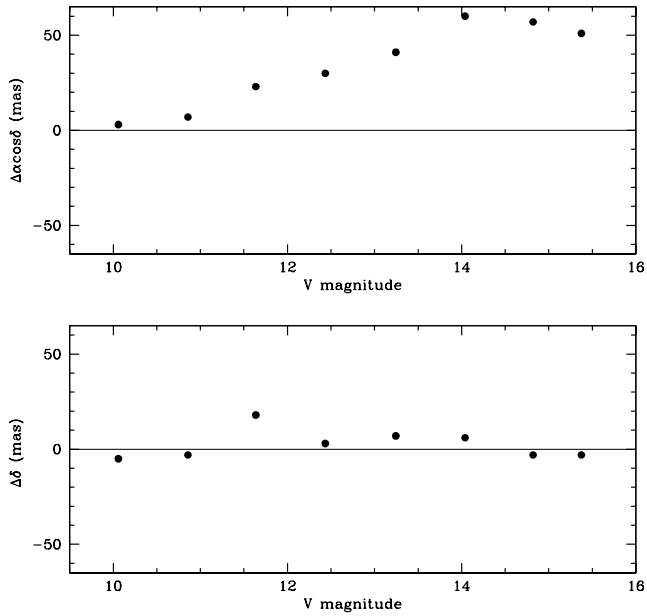

Fig. 3. Positional differences in the sense Valinhos minus Bordeaux as a function of magnitude.

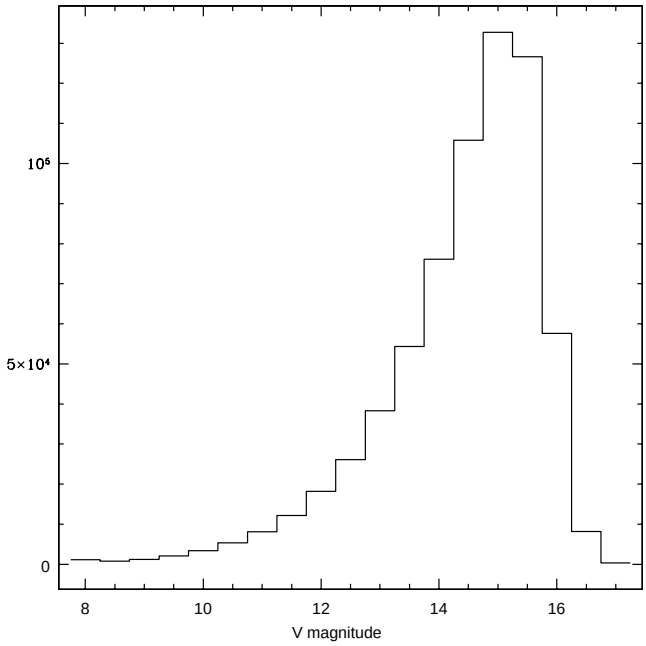

Fig. 4. Object distribution per visual magnitude in the BVMCcat.

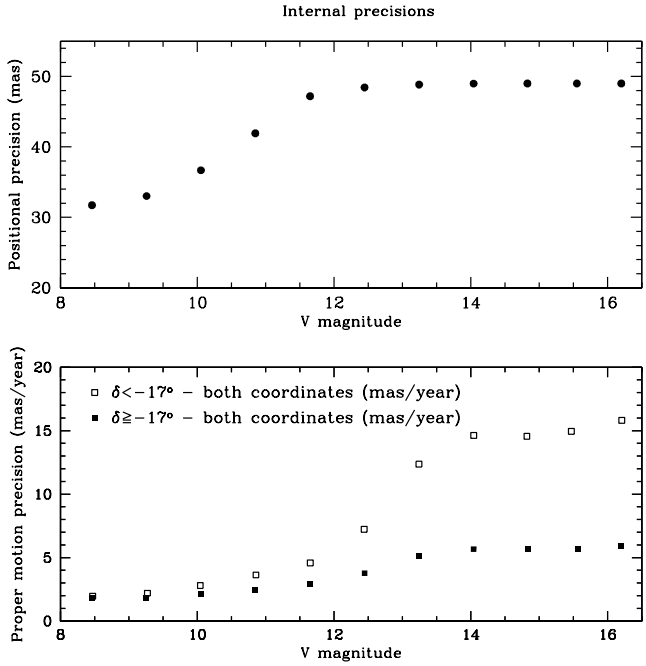

Fig. 5. Internal astrometric precisions of the BVMCcat as a function of magnitude.

For referencing, the other employed catalogues are presented as follows: SERC–J plates measured with the MAMA measuring machine (Guibert et al. 1983), PPM South (Bastian & Röser 1993), PPM North (Röser & Bastian 1998), USNO–A2.0 (Monet et al. 1998), TAC–2 (Zacharias & Zacharias 1999), and CPC–2 (Zacharias et al. 1999).

4. The BVMCcat

The BVMCcat contains 678 828 stars brighter than $V \sim 16.0$, observed at least 3 times with either the BMC or the VMC, whose distribution as a function of magnitude can be seen in Fig. 4.

A weighted least squares procedure was used to derive positions and proper motions. The adopted weights were taken from the precisions given by the employed material. On average, these values are: 250 mas for the USNO–A2.0, 100 mas for the TAC–2, 300 mas for the AC2000.2, 270 mas for the PPM-North, 110 mas for the PPM-South, 50 mas for the CPC–2 and 300 mas for the SERC–J plates. For the meridian positions, 50 mas was used (Rapaport et al. 2001; Teixeira et al. 2000), which is a good compromise between the internal precisions of the mean positions for the Bordeaux and Valinhos instruments.

Figure 5 depicts average internal precisions of the BVMCcat for mean positions (upper panel) and proper motions (lower panel) as a function of magnitude.

The profile presented by the upper panel of Fig. 5 reflects the decreasing number of participant catalogues for the position/proper motion determination and the larger (5 times) weight given to the meridian positions as compared to the one given to those from USNO–A2.0 and the SERC–J plates. Theoretically, they should be in accordance with external verifications (presented later in the text) at least within the optimal magnitude range for the BMC and VMC astrometry (Fig. 1). To the faintest magnitudes, mean positions and their respective epochs will be close to their meridian counterparts.

The lower panel of Fig. 5 depicts a different behaviour of proper motion accuracies, given by a declination threshold of $\delta = -17°$. As explained in Camargo et al. (2001), this is due to the USNO–A2.0, which is the only source of first epoch positions for objects fainter than $V \sim 13.0$. In USNO–A2.0 the mean epoch for objects with $\delta \leq -17°$ is 1980, and 1955 for those with $\delta > -17°$.

Table 3 explains the role of each column of the BVMCcat, given in Table 2.

5. External verifications of the BVMCcat

Three catalogues were employed to check the BVMCcat: the HIPPARCOS and TYCHO–2 catalogues, for the BVMCcat stars with $V \leq 12.0$, and UCAC1 (Zacharias et al. 2000), when available, for the fainter ones. All differences were obtained after transferring these reference positions, through their respective proper motions, to the epoch of the BVMCcat ones. Data derived from both meridian instruments are homogeneous after correction for the magnitude equation on the VMC right ascension system, so that no separate treatment will be provided.

5.1. Comparison with HIPPARCOS

The BVMCcat contains 2119 HIPPARCOS objects, out of which 1167 were selected by the criterion that eliminated those with $V < 8.0$ (in order to avoid saturated observations from the meridian instruments), with HIPPARCOS `MultFlag`[2] flag set (in order to avoid binary/multiple systems), as well as some

[2] HIPPARCOS' Double/Multiple Systems flag. For detailed information, please refer to ESA (1997).

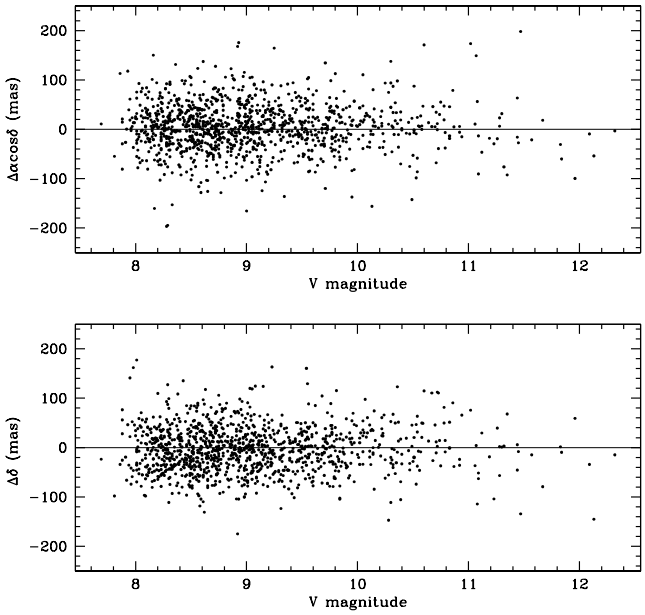

Fig. 6. Positional differences in the sense BVMCcat minus HIPPARCOS, as a function of magnitude, at the epoch of the BVMCcat. Upper panel: right ascension. Lower panel: declination.

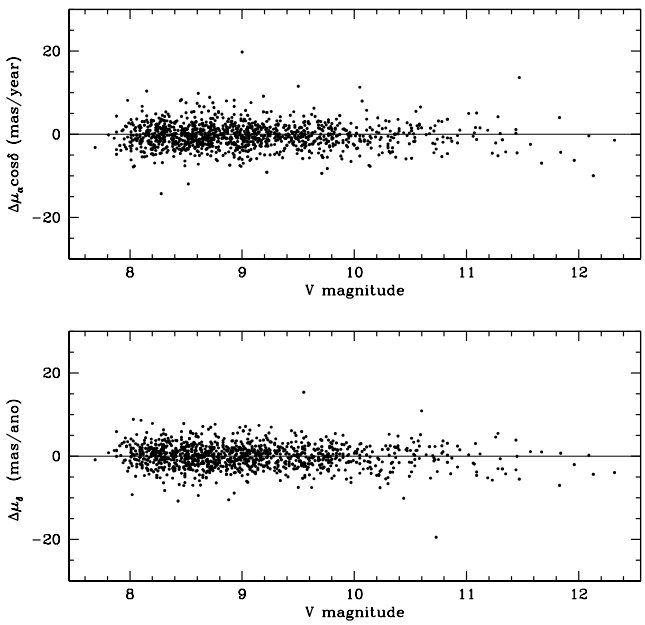

Fig. 7. Proper motion differences in the sense BVMCcat minus HIPPARCOS as a function of magnitude. Upper panel: right ascension. Lower panel: declination.

few remaining idiosyncratic points that failed to pass a 3σ filter in position, that is, whose modulus of the positional difference were greater than 3 times the root mean square (rms) of the differences in either coordinates.

Figures 6 and 7 depict the differences in the sense BVMCcat minus HIPPARCOS as a function of magnitude at the epoch of the BVMCcat, and Table 4 shows related quantities obtained from the rms of these differences.

Table 4. Statistical characteristics of the differences BVMCcat minus HIPPARCOS.

Objects	1167
$< \Delta\alpha\cos\delta >$	4
$< \Delta\delta >$	−4
$< \Delta\mu_\alpha\cos\delta >$	−0.4
$< \Delta\mu_\delta >$	−0.1
$\sigma_{\Delta\alpha\cos\delta}$	50
$\sigma_{\Delta\delta}$	50
$\sigma_{\Delta\mu_\alpha\cos\delta}$	3
$\sigma_{\Delta\mu_\delta}$	3

All units are in [mas] or [mas/year]. Comparisons were done at the epoch of the BVMCcat.

The quantities presented in the aforementioned table show an overall good agreement between the BVMCcat data and that of the HIPPARCOS catalogue.

The propagated errors[3] of HIPPARCOS at the epoch of the BVMCcat positions, about 10 mas, were considered negligible, so that we conclude that the BVMCcat external positional precision is about 50 mas within the magnitude interval $8.0 \leq V \leq 12.0$. The comparison of the BVMCcat proper motions with those from HIPPARCOS shows that, for objects with the AC2000.2 as the first epoch, the external error for the measurements in the BVMCcat is 3 mas/year.

5.2. Comparison with Tycho–2

The BVMCcat contains 45 394 objects in common with Tycho–2, whose differences in positions (at the epoch of the BVMCcat) and proper motions are depicted by Figs. 8 and 9 as a function of magnitude, after a 3σ filter in position.

Poor positional history within the employed catalogues and possible cross-identification difficulties contribute to the largest differences depicted in Fig. 9.

In Table 5, a more detailed comparison of position is shown, where a 3σ filter within each magnitude bin was applied. For the same objects presented in the aforementioned table, related quantities for the rms of the differences in proper motions are given in Table 6.

As in the comparison with HIPPARCOS, an overall good agreement between the positions is shown by Table 5, which corroborates the value of 50 mas for the BVMCcat external positional precision (lines 6 and 7 of Table 5) when $8.0 \leq V \leq 11.5$. External precision was obtained by subtracting from the $\sigma_{(\Delta\alpha\cos\delta,\Delta\delta)}$ values, as evaluated by the rms of the differences, the formal positional error of the Tycho–2 positions at the comparison epoch, as calculated from Høg et al. (2000).

For $V > 11.5$, one can notice a degradation of the external precision of the BVMCcat, which may result partly from Tycho–2 underestimated errors in its faintest branch, as pointed out in Rapaport et al. (2001) and supported later in the text (Sect. 5.3), by the comparison BVMCcat and UCAC1.

[3] According to relations 1.5.23, from Sect. 1.5 – "Transformation of Astrometric Data and Associated Error Propagation". For detailed information, please refer to ESA (1997).

Table 5. Statistical properties of the positional differences BVMCcat minus Tycho–2.

	V magnitude							
	8.0–8.5	8.5–9.0	9.0–9.5	9.5–10.0	10.0–10.5	10.5–11.0	11.0–11.5	11.5–12.0
Objects	571	963	1534	2456	3875	6113	9466	10491
$\sigma_{\Delta\alpha\cos\delta}$	65	56	47	47	48	60	89	125
$\sigma_{\Delta\delta}$	65	53	48	47	49	61	81	112
$< \Delta\alpha\cos\delta >$	1	6	2	0	−1	−2	−3	−2
$< \Delta\delta >$	1	−1	−1	−3	1	2	1	2
External precision in $\alpha\cos\delta$	64	54	44	44	37	52	56	103
External precision in δ	64	51	45	44	38	52	43	87

All astrometric units are in [mas]. External precisions are calculated by subtracting from the $\sigma_{(\Delta\alpha\cos\delta,\Delta\delta)}$ values the respective propagated Tycho–2 error at the BVMCcat epoch.

Table 6. Statistical properties of the proper motion differences BVMCcat minus Tycho–2.

	V magnitude							
	8.0–8.5	8.5–9.0	9.0–9.5	9.5–10.0	10.0–10.5	10.5–11.0	11.0–11.5	11.5–12.0
$\sigma_{\Delta\mu_\alpha\cos\delta}$	3	3	2	2	2	2	2	3
$\sigma_{\Delta\mu_\delta}$	3	3	2	2	2	2	2	2
$< \Delta\mu_\alpha\cos\delta >$	−0.2	−0.3	−0.4	−0.2	−0.1	−0.1	−0.2	−0.2
$< \Delta\mu_\delta >$	0.3	0.1	0.2	0.0	0.1	0.1	0.1	0.1

All astrometric units are in [mas/year]. The same objects from Table 5 are used.

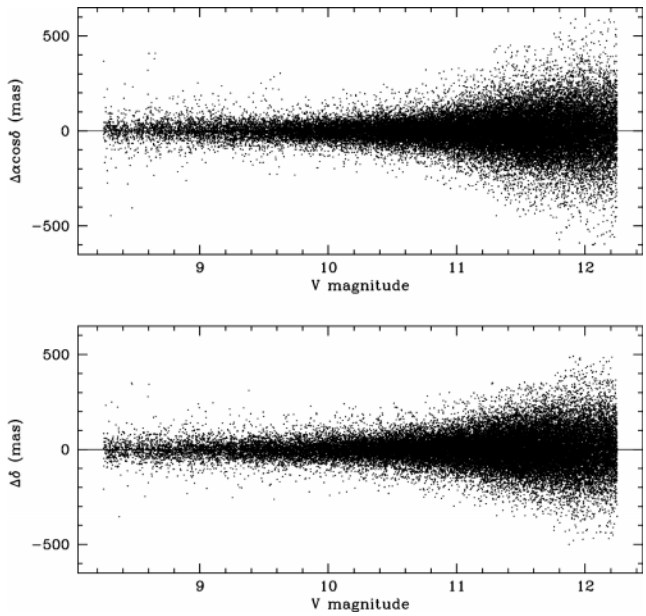

Fig. 8. Positional differences in the sense BVMCcat minus Tycho–2, as a function of magnitude, at the epoch of the BVMCcat. Upper panel: right ascension. Lower panel: declination.

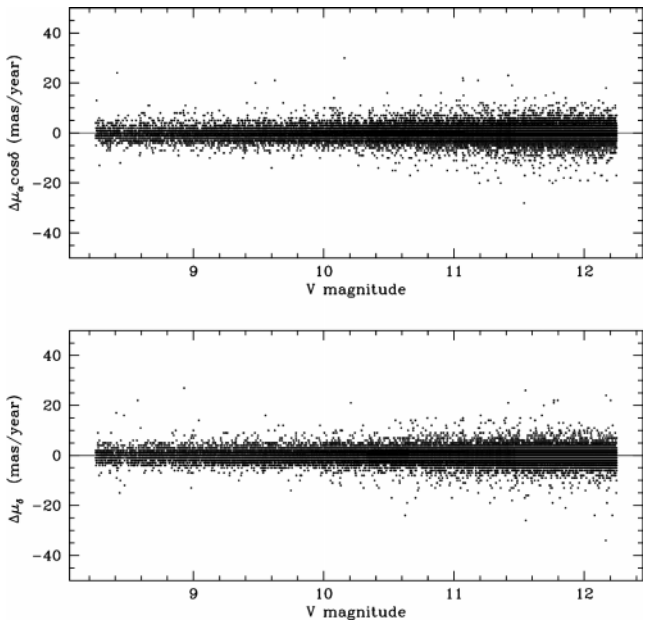

Fig. 9. Proper motion differences in the sense BVMCcat minus Tycho–2 as a function of magnitude. Upper panel: right ascension. Lower panel: declination.

From Table 6, we evaluate the BVMCcat external errors on proper motions as ∼2 mas/year within the interval $8.0 \leq V \leq 12.0$.

5.3. Comparison with UCAC1

The UCAC1 catalogue was employed to probe the BVMCcat results on fainter magnitudes, aiming at the objects fainter than $V = 12.0$. We should stress that, in this verification, only the data derived from the VMC was employed, that is, the predominantly southern declinations, since UCAC1 is only available in that hemisphere.

Table 7 provides a detailed view of this comparison. In it, as in Table 5, all differences in position were binned in intervals of 0.5 mag, and those above a 3σ filter in the respective bin were eliminated.

Table 7. Statistical properties of the positional differences BVMCcat minus UCAC1.

	V magnitude									
	11.0–11.5	11.5–12.0	12.0–12.5	12.5–13.0	13.0–13.5	13.5–14.0	14.0–14.5	14.5–15.0	15.0–15.5	15.5–16.0
Objects	1963	3043	4436	6143	8767	12200	16847	21224	20154	6878
$\sigma_{\Delta\alpha\cos\delta}$	49	52	55	58	65	71	81	100	129	141
$\sigma_{\Delta\delta}$	53	58	62	68	73	80	92	112	145	154
$< \Delta\alpha\cos\delta >$	−4	−6	−3	2	3	−6	−4	−2	1	2
$< \Delta\delta >$	−11	−11	−11	−9	−7	−6	−6	−6	−5	−9
External precision in $\alpha\cos\delta$	46	49	52	54	61	67	76	95	108	133
External precision in δ	51	55	59	65	70	77	89	108	141	147

All astrometric units are in [mas]. External precisions are calculated by subtracting from the $\sigma_{(\Delta\alpha\cos\delta,\Delta\delta)}$ values the respective propagated UCAC1 error at the BVMCcat epoch.

Table 8. Statistical properties of the proper motion differences BVMCcat minus UCAC1.

	V magnitude									
	11.0–11.5	11.5–12.0	12.0–12.5	12.5–13.0	13.0–13.5	13.5–14.0	14.0–14.5	14.5–15.0	15.0–15.5	15.5–16.0
$\sigma_{\Delta\mu_\alpha\cos\delta}$	5	7	7	6	7	5	5	6	8	8
$\sigma_{\Delta\mu_\delta}$	6	8	6	7	8	6	6	7	8	9
$< \Delta\mu_\alpha\cos\delta >$	−0.2	0.0	−0.1	0.0	0.1	−0.4	−0.2	−0.1	0.1	0.1
$< \Delta\mu_\delta >$	0.5	0.6	0.1	−0.2	−0.3	−0.3	−0.4	−0.4	−0.4	−0.6

All astrometric units are in [mas/year]. The same objects from Table 7 are used.

External precision is evaluated to 50–60 mas up to $V = 13.5$, well within the BMC and VMC optimal magnitude interval for astrometry (Fig. 1). This external precision reaches 140 mas for the fainter objects ($V \geq 15.0$).

The external precisions presented for the magnitude interval $11.5 \leq V \leq 12.0$, when compared to those in the same interval of Table 5, support a possible underestimation of the Tycho–2 errors for right ascensions within this magnitude interval.

To the same objects presented in Table 7, the rms of the differences in proper motions (Table 8) is 7 mas/year for both coordinates ($11.0 \leq V \leq 16.0$), and no systematic deviation was detected. Such an estimation, however, reflects that both BVMCcat and UCAC1 use the same first epoch positions (USNO–A2.0) to derive most of these quantities.

6. Conclusions

The BVMCcat extends the ICRF to the optical domain in zones of special astronomical interest, and the overall agreement between the BVMCcat data and that of well-known astrometric material enables it to serve as a reference catalogue for small field astrometry as well as to provide kinematical parameters for astrophysical studies within the limits of ground-based astrometry.

The collaboration of northern (Bordeaux) and southern (Valinhos) Observatories allowed a more efficient sky coverage and a larger number of entries for the BVMCcat, as compared to our previous work (Camargo et al. 2001).

The external comparisons showed that no significant systematic trend was found either in positions or proper motions. The external errors of the BVMCcat are 50–60 mas for positions on both coordinates when $V \leq 13.5$ and 70–140 mas for fainter magnitudes ($13.5 \leq V < 16.0$). For proper motions, external errors are 3 mas/year when an AC2000.2 position is present as first epoch ($V \lesssim 13.0$) reaching probably 15 mas/year for the faintest objects at southern declinations, as suggested by the internal error degradation (Fig. 5, lower panel).

Acknowledgements. The authors wish to express their thanks to the computer service of IAG/USP (Department of Astronomy) and of the Bordeaux Observatory, for their valuable help and patience during data-processing. The authors are also indebted to the observers of both Brazilian and French meridian circles. J. I. B. Camargo expresses his thanks to Dr. C. L. Dal Ri Barbosa and Dr. G. M. Tanco, for their help with the 2MASS data. The authors are thankful to Dr. G. Daigne, Dr. C. Soubiran and J. P. Périé for suggestions and contributions. A partial financial support from FAPESP, CAPES, PRONEX and CNRS is gratefully acknowledged. This work has made use of the NASA's Astrophysics Data System Abstract Service. This publication makes use of data products from the Two Micron All Sky Survey, which is a joint project of the University of Massachusetts and the Infrared Processing and Analysis Center/California Institute of Technology, funded by the National Aeronautics and Space Administration and the National Science Foundation. This research has made use of the SIMBAD database, operated at CDS, Strasbourg, France. The authors express their thanks to the referee, Dr. C. Ma, for fruitful suggestions and corrections. J. I. B. Camargo is supported by CNPq – Brazil.

References

Bastian, U., & Röser, S. 1993, The PPM–South Catalogue (Heidelberg: Spektrum, Akademischer Verlag)

Benevides-Soares, P. 2003, private communication

Camargo, J., Teixeira, R., Benevides-Soares, P., et al. 2001, A&A, 375, 308

de Vegt, C., Hindsley, R., Zacharias, N., et al. 2001, AJ, 121, 2815
Dominici, T., Teixeira, R., Horvath, J., Medina Tanco, G., & Benevides-Soares, P. 1999, A&AS, 136, 261
ESA. 1997, The HIPPARCOS and Tycho Catalogues, ESA SP
Feissel, M., & Mignard, F. 1998, A&A, 331, L33
Fricke, W., Schwan, H., Lederle, T., et al. 1988, Fifth Fundamental Catalogue – Basic Fundamental Stars (Veröffentlichungen des Astronomisches Rechen-Institut, Heidelberg), 32
Guibert, J., Charvin, P., & Stoclet, P. 1983, in Proc. of the 78th Colloq. of the IAU, 165
Høg, E., Fabricius, C., Makarov, V., et al. 2000, A&A, 355, L27
Johnston, K., & de Vegt, C. 1999, ARA&A, 37, 97
Ma, C., Arias, E., Eubanks, T., et al. 1998, AJ, 116, 516
Monet, D., Bird, A., Canzian, B., et al. 1998, in USNOA–V2.0. A Catalog of Astrometric Standards
Rapaport, M., Le Campion, J.-F., Soubiran, C., et al. 2001, A&A, 376, 325
Röser, S., & Bastian, U. 1998, A&AS, 74, 449
Teixeira, R., Ducourant, C., Sartori, M., et al. 2000, A&A, 361, 1143
Urban, S., Corbin, T., Wycoff, G., et al. 1998, AJ, 115, 1212
Urban, S., Corbin, T., Wycoff, G. et al. 2001, AAS, 1991, 2904
Viateau, B., Réquième, Y., Le Campion, J., et al. 1999, A&AS, 134, 173
Zacharias, N., Urban, S., Zacharias, M., et al. 2000, AJ, 120, 2131
Zacharias, N., & Zacharias, M. 1999, AJ, 118, 2503
Zacharias, N., Zacharias, M., & de Vegt, C. 1999, AJ, 117, 2895

Online Material

Table 1. List of strips observed by the meridian circles.

Target	#Objects	$\frac{\sigma_\alpha \cos\delta \quad \sigma_\delta}{[\mathrm{mas}]}$	$\frac{\alpha}{[\mathrm{J2000}]}$	$\frac{\delta}{[\mathrm{J2000}]}$	$\frac{\mathrm{mag}}{[V]}$	Nobs
Valinhos zones						
NGC 7772	292	075 084	00 00 05.0	+16 16 01		14
C 0001−302	220	081 105	00 01 56.5	−30 06 38		05
ICRF J001031.0+105829	261	113 117	00 10 31.0	+10 58 30	15.4	10
ICRF J004959.4−573827	209	094 101	00 49 59.5	−57 38 27	18.5	13
VV96 J005334.9+124136	447	080 114	00 53 34.9	+12 41 36	15.7	10
ICRF J011205.8+224438	660	070 091	01 12 05.8	+22 44 39	20.0	13
ICRF J013305.7−520003	176	065 088	01 33 05.8	−52 00 04		06
UV Cet	137	113 118	01 36 27.0	−17 57 30		05
ICRF J015002.6−072548	156	122 118	01 50 02.7	−07 25 48	15.6	06
ICRF J023951.2+041621	273	110 127	02 39 51.3	+04 16 21	18.5	08
ICRF J024008.1−230915	552	098 104	02 40 08.2	−23 09 16	16.6	10
ICRF J024104.7−081520	382	075 092	02 41 04.8	−08 15 21	12.3	06
J032021.2−192631	85	117 143	03 20 21.2	−19 26 31		04
HD 23158	289	081 126	03 47 15.4	+24 15 57		04
NGC 1778	104	137 157	05 00 48.1	+36 59 28		05
ICRF J053850.3−440508	467	076 094	05 38 50.4	−44 05 09	16.5	08
NGC 2323	214	110 118	07 03 51.6	−08 15 58		04
ICRF J073807.3+174218	1002	074 099	07 38 07.4	+17 42 19	16.2	09
NGC 2506	1062	076 100	08 03 54.6	−10 47 08		07
YZ Cnc	292	101 117	08 09 39.8	+28 08 20		06
ICRF J081108.8−492943	1580	076 097	08 11 08.8	−49 29 43		06
XY Pup	1454	093 097	08 11 53.5	−11 59 05		05
C 0810−277	5534	082 094	08 12 29.0	−28 12 35		04
RX Pup	819	068 098	08 13 37.8	−41 42 28		06
AC Cnc	197	110 127	08 43 59.5	+12 50 40		10
NGC 2682	938	082 094	08 51 56.7	+11 59 40		07
WY Cnc	308	073 096	08 59 28.6	+26 41 01		07
ICRF J091552.4+293324	222	075 091	09 15 52.4	+29 33 24	16.4	05
ICRF J092129.3−261843	948	082 097	09 21 29.4	−26 18 34	18.4	08
C 0939−536	6004	086 094	09 45 18.7	−53 51 44		08
Chamaeleon	1094	090 095	09 49 35.8	−76 49 12		14
C 0949−529	3789	078 101	09 55 42.5	−53 13 37		09
AL Leo	95	105 128	09 56 59.4	+18 17 30		04
ICRF J100159.9−443800	1196	094 099	10 01 59.9	−44 38 01	17.0	04
ICRF J101353.4+244916	264	094 115	10 13 53.4	+24 49 16	16.6	10
IC 2581	4211	034 041	10 24 51.3	−57 39 33		10
ICRF J103502.1−201134	535	065 076	10 35 02.2	−20 11 34	19.0	09
ICRF J103716.0−293402	1010	070 091	10 37 16.1	−29 34 03	16.5	11
TW Hya	1041	041 048	10 55 25.1	−34 43 26		20
ICRF J110331.5−325116	253	073 087	11 03 31.5	−32 51 17	16.3	08

Table 1. continued.

Target	#Objects	$\frac{\sigma_\alpha \cos\delta \quad \sigma_\delta}{[\mathrm{mas}]}$	$\frac{\alpha}{[\mathrm{J2000}]}$	$\frac{\delta}{[\mathrm{J2000}]}$	$\frac{\mathrm{mag}}{[V]}$	Nobs
ICRF J110427.3+381231	95	106 139	11 04 27.3	+38 12 32	12.9	08
PMN J1109−3732	559	074 089	11 09 48.0	−37 30 37		06
Chamaeleon	805	056 067	11 13 48.9	−76 32 27		06
PMN J1117−6156	3972	070 090	11 16 50.4	−61 54 47		05
NGC 3680	1410	035 051	11 24 34.9	−43 15 09		10
ICRF J113143.2−581853	2437	088 100	11 31 43.3	−58 18 53		10
SY Mus	2481	106 110	11 35 45.1	−65 26 41		05
TW Vir	209	077 110	11 43 07.3	−04 24 31		05
ICRF J114701.3−381211	911	087 085	11 47 01.4	−38 12 11	16.2	12
ICRF J115931.8+291443	228	091 100	11 59 31.8	+29 14 44	14.4	08
TXS 1217−322	711	089 090	12 20 02.6	−32 34 14		08
ICRF J122906.6+020308	407	096 095	12 29 06.7	+02 03 09	12.9	09
FL Vir	119	116 124	12 32 45.0	+09 01 00		04
V850 Cen	1889	098 109	13 00 43.1	−61 37 34		08
Chamaeleon	482	046 044	13 01 35.4	−76 39 33		08
DT Vir	136	120 131	13 04 05.8	+12 21 59		07
ICRF J130533.0−103319	261	087 098	13 05 33.0	−10 33 19	15.2	09
V803 Cen	1187	109 110	13 22 00.2	−41 44 15		05
ICRF J132304.2−445233	1833	066 080	13 23 04.2	−44 52 34		10
ICRF J133237.5−664650	5041	080 095	13 32 37.5	−66 46 50		09
C 1333−619	5533	088 089	13 35 39.9	−62 10 38		11
ICRF J133752.4−650924	3474	084 104	13 37 52.4	−65 09 25		10
RW Hya	329	118 124	13 44 00.2	−25 22 34		05
BH Vir	211	115 125	13 54 07.6	−01 40 04		05
ICRF J135704.4+191907	436	077 094	13 57 04.4	+19 19 07	16.0	11
ICRF J135900.1−415252	1478	065 080	13 59 00.2	−41 52 53	15.9	07
ICRF J140700.3+282714	325	098 105	14 07 00.4	+28 27 15	15.4	12
ICRF J142700.3+234800	233	089 092	14 27 00.4	+23 48 00	15.0	10
NGC 5606	4014	091 093	14 30 13.6	−59 39 33		06
ICRF J143809.4−220454	960	080 086	14 38 09.5	−22 04 55	17.9	12
Lupus	3674	063 077	14 38 37.0	−39 24 28		23
ICRF J144516.4+095836	221	076 092	14 45 16.5	+09 58 36	17.8	05
ICRF J144553.3−162901	117	072 082	14 45 53.4	−16 29 01		08
V822 Cen	668	081 101	14 57 45.6	−31 40 11		04
NGC 5823	1783	047 056	15 02 46.0	−55 34 49		09
ICRF J151344.8−101200	454	110 114	15 13 44.8	−10 12 00	18.5	06
ICRF J151656.7+193212	305	074 094	15 16 56.8	+19 32 13	18.7	14
C 1511−588	2175	084 111	15 17 22.8	−59 06 54		11
ICRF J151741.8−242219	1640	075 094	15 17 41.8	−24 22 19	14.8	10
ICRF J153452.4+013104	345	074 090	15 34 54.5	+01 31 04	18.0	04
Lupus	4683	073 086	15 42 46.6	−39 18 47		17

Table 1. continued.

Target	#Objects	$\frac{\sigma_\alpha \cos\delta \quad \sigma_\delta}{[\mathrm{mas}]}$	$\frac{\alpha}{[\mathrm{J2000}]}$	$\frac{\delta}{[\mathrm{J2000}]}$	$\frac{\mathrm{mag}}{[V]}$	Nobs
HT Lup	799	088 111	15 44 58.0	−34 16 54		04
HD 143329	219	105 116	15 54 22.7	+26 38 53		08
HD 143006	537	112 116	15 56 32.7	−22 56 20		08
GQ Lup	1743	082 105	15 56 43.0	−35 39 53		22
RU Lup	271	103 149	15 56 49.4	−37 45 00		06
PLUTO−97	2040	073 093	15 59 03.0	−08 24 05		12
PLUTO−96	1677	075 076	16 02 33.3	−07 19 37		27
HBC 630	706	089 098	16 09 03.8	−19 04 49		07
VV96 J161033.4+111531	766	101 097	16 10 33.5	+11 15 31		12
PLUTO−98	1234	121 126	16 29 17.9	−09 16 52		11
Oph + Upper *Sco*	1419	053 069	16 34 45.9	−24 10 34		18
PLUTO-99	364	106 123	16 40 12.3	−10 04 10		06
AK Sco	3197	089 109	16 48 48.3	−36 54 00		12
HBC 652	274	114 116	16 49 04.8	−14 11 10		04
Oph + Upper *Sco*	1707	098 107	16 53 36.4	−27 26 13		04
HD 326823	602	111 126	17 06 03.4	−42 37 31		08
V455 Sco	271	124 139	17 06 52.1	−34 04 44		04
Ross 868	138	124 126	17 18 32.3	+26 29 41		06
ICRF J172341.0−650036	1898	057 067	17 23 41.0	−65 00 37	15.5	10
RV Oph	369	113 123	17 34 05.0	+07 15 49		07
IC 4665	1803	092 110	17 39 54.6	+05 48 16		05
LE – bulge	6008	088 106	17 48 41.7	−39 25 43		08
LF – bulge	6386	094 109	17 54 08.6	−37 33 36		08
BA – bulge	8890	080 097	17 57 51.4	−28 45 41		08
BB – bulge	9124	098 107	18 00 24.6	−29 13 21		06
YY Her	235	126 138	18 14 42.6	+20 58 58		03
BD−11 4586	465	100 107	18 18 12.2	−11 18 13		06
BH – bulge	6333	093 113	18 22 51.5	−33 30 16		07
LS – bulge	5769	088 101	18 27 25.7	−24 33 41		07
BI – bulge	6061	089 104	18 27 30.8	−33 56 53		09
VCLS 121	555	120 124	18 45 45.1	−03 47 05		05
S CrA	1669	079 087	18 57 56.4	−36 57 24		15
CD− 35 13069	1840	085 098	18 59 28.1	−35 39 54		04
Gliese 748	2637	089 107	19 13 26.1	+02 53 19		08
BF Cyg	3781	096 107	19 19 25.7	+29 46 17		11
AS 353A 7	1854	083 112	19 19 57.1	+11 02 27		08
V1370 Aql	1437	109 115	19 20 06.0	+14 52 57		08
ICRF J192451.0−291430	2755	064 089	19 24 51.1	−29 14 30	18.2	12
ICRF J193006.1−605609	838	094 097	19 30 06.2	−60 56 09	21.5	11
OO Aql	3872	110 105	19 47 04.2	+09 18 25		09
NGC 6834	1962	059 066	19 52 31.8	+29 24 44		09

Table 1. continued.

Target	#Objects	$\sigma_\alpha \cos\delta$ σ_δ [mas]	α [J2000]	δ [J2000]	mag [V]	Nobs
C 1950+182	3875	070 086	19 55 50.5	+18 19 49		14
ICRF J200925.3−484953	1485	070 100	20 09 25.4	−48 49 54	13.4	10
V794 Aql	132	116 132	20 15 49.0	−03 39 25		04
HD 340611	2144	079 097	20 34 05.4	+25 03 50		13
W Del	959	105 117	20 35 27.0	+18 15 53		04
ER Del	1852	080 090	20 38 27.0	+08 41 39		11
ICRF J205616.3−471447	715	088 096	20 56 16.4	−47 14 48	19.1	11
NGC 6994	730	027 035	21 01 24.4	−12 38 35		09
J210933.1−411020	417	055 072	21 09 33.2	−41 10 21	21.0	12
GJ 821	687	070 082	21 12 00.5	−13 18 02		15
W Equ	843	124 123	21 16 10.1	+12 22 10		06
ICRF J213135.2−120704	592	095 094	21 31 35.3	−12 07 05	16.1	09
ICRF J215705.9−694123	652	095 139	21 57 06.6	−69 41 24	13.8	06
ICRF J215852.0−301332	806	066 091	21 58 52.1	−30 13 32	13.1	11
ICRF J220314.9+314538	1793	106 112	22 03 15.0	+31 45 38	15.6	06
ICRF J220743.7−534633	456	089 094	22 07 43.7	−53 46 34	18.0	10
ICRF J221852.0−033536	829	092 101	22 18 52.0	−03 35 36	16.4	09
ICRF J225357.7+160853	387	069 109	22 53 57.7	+16 08 54	16.1	13
VV96 J225405.9−173455	684	089 087	22 54 05.9	−17 34 55		10
ICRF J225717.3+074312	494	108 117	22 57 17.3	+07 43 12	16.4	07
ICRF J225805.9−275821	249	099 113	22 58 06.0	−27 58 21	16.8	08
ICRF J232917.7−473019	206	097 099	23 29 17.7	−47 30 19	16.8	09
ICRF J233040.8+110018	395	062 084	23 30 40.9	+11 00 19	18.1	12
EQ Peg	102	121 111	23 31 21.6	+19 55 31		03
ICRF J234636.8+093045	557	077 116	23 46 36.8	+09 30 46	16.0	12
Bordeaux zones						
V633 Cas	3095	097 077	00 12 46.2	+58 49 43		06
ICRF J001031.0+105829	1111	060 072	00 21 33.3	+10 56 10	15.4	10
ICRF J005041.3−092905	1210	060 076	01 14 26.9	−09 30 07	17.4	09
ICRF J011205.8+224438	2345	053 062	01 19 09.1	+22 42 29	15.7	25
ICRF J011935.0+321050	2819	061 067	01 49 17.5	+32 10 27	16.0	16
ICRF J015002.6−072548	1015	044 053	01 58 49.3	−07 27 18	15.6	33
RNO 6	6707	087 076	02 21 48.3	+55 21 49		07
ICRF J023838.9+163659	4492	063 070	02 37 27.5	+16 28 00	15.5	23
0129+428	5385	081 070	02 37 48.4	+43 02 01		22
LkHA262	1253	074 084	02 56 06.6	+20 05 00		05
ICRF J031948.1+413042	9457	067 062	03 18 48.6	+41 29 52	12.5	19
RNO 13	493	082 091	03 23 44.4	+30 38 37		06
LZK 4	719	078 081	03 27 28.7	+31 11 29		03
XY Per	1138	086 091	03 47 00.0	+38 56 26		06
IP Per	2088	075 081	03 48 18.8	+32 23 01		09

Table 1. continued.

Target	#Objects	$\frac{\sigma_\alpha \cos\delta \quad \sigma_\delta}{[\mathrm{mas}]}$	$\frac{\alpha}{[\mathrm{J2000}]}$	$\frac{\delta}{[\mathrm{J2000}]}$	$\frac{\mathrm{mag}}{[V]}$	Nobs
0310+0122	225	107 123	03 53 05.9	+01 34 16		04
ICRF J040748.4−121136	1101	059 064	04 05 29.1	−12 13 41	14.9	18
ICRF J033930.9−014635	1385	074 087	04 07 39.3	−01 33 36	18.4	04
PP 13	460	096 105	04 08 31.4	+38 07 05		06
BP Tau	1728	077 083	04 22 50.0	+29 06 42		06
DI Tau	290	085 093	04 30 07.4	+26 32 16		06
ICRF J043311.0+052115	5626	061 069	04 45 46.7	+05 21 24	15.1	25
DS Tau	1125	083 087	04 50 34.1	+29 24 49		06
V836 Tau	2070	076 082	05 05 28.7	+25 22 33		07
LkHA 333	1983	068 083	05 05 42.5	−03 19 48		04
UX Ori	1791	061 071	05 22 27.4	−03 47 44		06
PQ Ori	2761	059 071	05 43 56.5	−02 21 11		12
V523 Ori	1638	081 100	05 45 25.2	−01 22 35		03
V350 Ori	2279	056 066	05 49 33.9	−09 43 35		09
ICRF J060752.6+672055	592	107 088	06 09 15.4	+67 20 29	20.6	04
RNO 66	1822	063 074	06 09 18.0	−06 55 53		07
V625 Ori	3298	074 080	06 12 52.7	+08 56 43		03
W84	9249	071 081	06 30 19.7	+09 40 26		06
0647+250	19993	058 057	06 30 50.3	+25 04 18		23
MO Mon	4684	073 083	06 35 18.4	+09 21 06		06
Z CMa	2420	068 079	07 00 24.6	−11 28 26		06
ICRF J073807.3+174218	6928	045 049	07 37 24.9	+17 40 55	16.2	38
1ES0806+524	1006	073 066	07 50 06.6	+52 20 04		18
ICRF J075706.6+095634	3775	057 060	07 56 41.3	+09 55 48	15.0	16
ICRF J082057.4−125859	3376	074 086	08 23 41.5	−13 00 30	15.0	04
OJ287	7473	043 047	08 27 18.7	+20 03 59		53
ICRF J091552.4+293324	1633	065 069	09 31 53.0	+29 33 21	16.4	16
1011+496	1565	064 056	09 57 10.8	+49 27 44		23
ICRF J095820.9+322402	957	077 067	09 59 25.1	+32 24 16	15.8	09
ICRF J110427.3+381231	1728	058 053	11 13 44.5	+38 12 50	12.9	54
1ES1113+432	233	084 081	11 30 40.7	+42 58 18		08
ICRF J115019.2+241753	609	059 065	11 59 16.2	+24 17 56	15.7	14
ICRF J115931.8+291443	459	064 070	11 59 31.6	+29 15 12	14.4	21
ICRF J123049.4+122328	2485	071 072	12 30 03.2	+12 28 08	12.9	13
ON231	404	094 098	12 37 24.1	+28 13 29		03
ICRF J130533.0−103319	779	090 096	12 59 07.1	−10 26 51	15.2	06
1ES1255+244	362	074 092	13 00 48.0	+24 12 17		03
ICRF J125614.2+565225	353	084 067	13 07 06.7	+56 52 39	13.8	13
ICRF J131028.6+322043	1631	057 060	13 19 29.6	+32 21 03	15.2	19
ICRF J135704.4+191907	1712	060 065	13 45 24.4	+19 18 53	16.0	38
1400+162	2653	059 063	13 59 57.3	+16 02 11		12

Table 1. continued.

Target	#Objects	$\frac{\sigma_\alpha \cos\delta \quad \sigma_\delta}{[\mathrm{mas}]}$	$\frac{\alpha}{[\mathrm{J2000}]}$	$\frac{\delta}{[\mathrm{J2000}]}$	$\frac{\mathrm{mag}}{[V]}$	Nobs
ICRF J140700.3+282714	926	072 081	14 05 52.7	+28 26 37	15.4	09
RXJ1412.2	1327	070 085	14 11 20.8	−16 30 12		06
RXJ1419.3	552	091 107	14 15 49.4	−23 22 44		04
ICRF J141946.5+542314	1211	069 058	14 25 14.9	+54 22 53	15.7	25
ICRF J142700.3+234800	1242	059 068	14 33 31.1	+23 47 40	15.0	06
1517+656	1664	075 054	15 17 23.3	+65 24 40		59
1553+113	5335	042 050	15 54 59.1	+11 08 15		49
ICRF J164258.8+394836	2855	055 053	16 52 00.8	+39 47 05	16.0	39
1722+119	15521	047 054	17 30 03.1	+11 52 21		66
LkHA 122	8607	082 092	18 00 50.8	−22 53 58		07
BD−10 4662	5012	076 088	18 20 31.5	−10 11 19		06
VV Ser	5535	067 080	18 25 25.8	+00 02 39		07
Coku Ser G6	5257	061 072	18 27 41.0	+00 29 29		07
LkHA 118	29348	080 092	18 42 46.3	−24 18 40		08
AS 310	13588	061 072	18 50 32.8	−04 58 25		16
FH Aql	28283	056 067	19 01 02.8	−05 36 50		15
WW Vul	15200	059 066	19 07 03.4	+21 11 45		15
Par 21	31525	061 071	19 21 41.1	+09 37 48		13
LHA 483−41	14181	080 086	19 22 50.6	+23 52 36		07
V536 Aql	27734	068 080	19 41 14.6	+10 29 34		08
1548C27	15796	064 071	19 57 22.8	+23 23 15		11
1ES1959+650	5259	078 060	19 58 42.6	+65 08 33		72
V1685 Cyg	10044	059 058	20 27 39.9	+41 20 37		20
2032+107	7621	055 066	20 32 25.9	+10 51 53		18
LkHA 168	7222	069 068	20 45 32.3	+44 31 11		09
LkHA 191	9099	067 065	20 55 35.1	+43 50 05		14
LkHA 321	4004	081 076	20 55 59.7	+49 50 50		06
BD+41 3731	10758	069 063	21 02 44.0	+42 14 28		16
LkHA 324	9583	078 075	21 15 26.9	+50 18 31		08
V1082 Cyg	13809	071 076	21 30 36.5	+43 20 50		06
LkHA 349	5889	083 068	21 35 22.6	+57 31 48		10
BD+46 3471	15319	066 064	21 46 04.2	+47 21 50		08
ICRF J220314.9+314538	7586	052 057	21 59 20.6	+31 46 08	15.6	21

Table 1. continued.

Target	#Objects	$\frac{\sigma_\alpha \cos\delta \quad \sigma_\delta}{[\mathrm{mas}]}$	$\frac{\alpha}{[\mathrm{J2000}]}$	$\frac{\delta}{[\mathrm{J2000}]}$	$\frac{\mathrm{mag}}{[V]}$	Nobs
ICRF J220243.2+421639	10808	060 061	22 05 50.5	+42 16 32	14.7	33
LkHA 233	11130	057 057	22 43 04.4	+40 41 46		18
DI Cep	9224	077 059	22 45 56.6	+58 44 28		17
J2253+1615	4501	047 051	22 59 54.4	+16 11 27		41
1ES2344+514	21692	062 054	23 30 24.7	+51 43 48		61
BM And	10472	077 074	23 39 36.3	+48 23 39		06

Target = ICRF name or other identifier of the target object; Objects = Total number of selected objects in the region: 3 or more observations in each coordinate and $\sigma_{(\alpha\cos\delta,\,\delta)}$ less than or equal 250 mas; $\frac{\sigma_\alpha \cos\delta \quad \sigma_\delta}{[\mathrm{mas}]}$ = Mean, in units of milliarc seconds to both coordinates, for the positional precision of the objects computed in the 2nd column; $\frac{\alpha}{[\mathrm{J2000}]}$ e $\frac{\delta}{[\mathrm{J2000}]}$ = Approximate central coordinates of the strips; V = V mag as given in the ICRF; Nobs = Number of observations of the target region.
Zones dimensions are typically 28′ in declination and 80^{m} in right ascension to the BMC and 13′ in declination and 40^{m} in right ascension to the VMC.

Table 3. Explanation of the columns in Table 2.

Field	Unit	Explanation
RA	[hour min sec]	right ascension, ICRS, for Epoch RA
DE	[deg ′ ″]	declination, ICRS, for Epoch DE
$\mu_\alpha \cos\delta$	[mas/year]	proper motion in right ascension, ICRS
μ_δ	[mas/year]	proper motion in declination, ICRS
Mag: meridian	[V]	meridian circle V magnitude
Mag: B Tycho-2	[B]	Tycho-2 B magnitude
Mag: V Tycho-2	[V]	Tycho-2 V magnitude
Mag: J 2MASS	[J]	2MASS J magnitude
Mag: H 2MASS	[H]	2MASS H magnitude
Mag: K 2MASS	[K]	2MASS K magnitude
Epoch RA	[year−1900]	epoch of right ascension, minus 1900
Epoch DE	[year−1900]	epoch of declination, minus 1900
ΔT	[year]	largest time interval for proper motion calculation
$\sigma_\alpha \cos\delta$	[mas]	precision in RA
σ_δ	[mas]	precision in DE
$\sigma_{\mu_\alpha} \cos\delta$	[mas/year]	precision in $\mu_\alpha \cos\delta$
σ_{μ_δ}	[mas/year]	precision in μ_δ
Nobs		number of observations in RA and DE
HIP		HIPPARCOS number
Tycho–2[1]		Tycho–2 number
AC		AC2000.2 number
Source[2]	[B/V, A, U, P, T, C, E]	employed astrometric catalogues for mean position and proper motion derivation

[1] An * present right after the Tycho–2 number indicates that the object is not contained in the Tycho–1.
[2] B to BMC or V to VMC; A = AC2000.2; U = USNO–A2.0; P = PPM; T = TAC–2; C = CPC–2; E = ESO plates.